



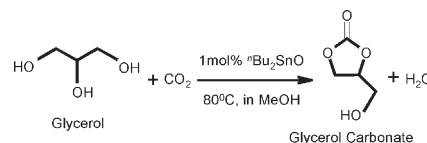
Contents

Jimil George, Yogesh Patel, S. Muthukumar Pillai, Pradip Munshi

Journal of Molecular Catalysis A: Chemical 304 (2009) 1

Methanol assisted selective formation of 1,2-glycerol carbonate from glycerol and carbon dioxide using ${}^n\text{Bu}_2\text{SnO}$ as a catalyst

Selective formation of 1,2-glycerol carbonate is observed in direct carbonation of glycerol with CO_2 using 1 mol% ${}^n\text{Bu}_2\text{SnO}$ as a true catalyst in presence of methanol. The catalyst possesses turnover number of 35, much higher than literature reported stoichiometric values. Identification of the intermediates by IR, NMR and mass spectral studies lead to describe reaction path.

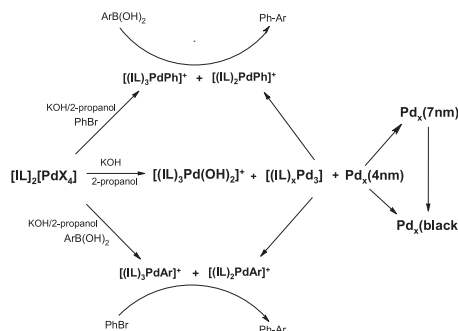


W. Zawartka, A. Gniewek, A.M. Trzeciak, J.J. Ziótkowski, J. Pernak

Journal of Molecular Catalysis A: Chemical 304 (2009) 8

Pd^{II} square planar complexes of the type $[\text{IL}]_2[\text{PdX}_4]$ as catalyst precursors for the Suzuki–Miyaura cross-coupling reaction. The first *in situ* ESI-MS evidence of $[(\text{IL})_x\text{Pd}_3]$ clusters formation

In situ ESI-MS evidence of $[\text{Pd}^0]_x$ nanoparticles formation and stabilization with ionic liquids during Suzuki–Miyaura reaction catalyzed with $[\text{IL}]_2[\text{PdX}_4]$ precursors.

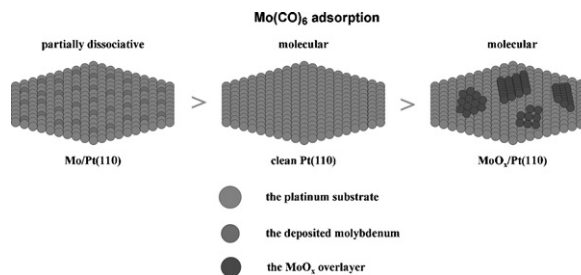


Zhiqian Jiang, Lingshun Xu, Weixin Huang

Journal of Molecular Catalysis A: Chemical 304 (2009) 16

Adsorption and reaction of $\text{Mo}(\text{CO})_6$ on chemically modified Pt(1 1 0) model surfaces

$\text{Mo}(\text{CO})_6$ molecularly adsorbs on Pt(1 1 0) and $\text{MoO}_x/\text{Pt}(1\ 1\ 0)$ at cryogenic temperature, however, undergoes partial dissociation on $\text{Mo}/\text{Pt}(1\ 1\ 0)$. $\text{Mo}/\text{Pt}(1\ 1\ 0)$ more strongly donates electrons to adsorbates than Pt(1 1 0) and $\text{MoO}_x/\text{Pt}(1\ 1\ 0)$, and thus exhibits a higher reactivity toward $\text{Mo}(\text{CO})_6$. The interaction of CO ligands in $\text{Mo}(\text{CO})_6$ with the metal surface is proposed to determine the adsorption behavior of $\text{Mo}(\text{CO})_6$.

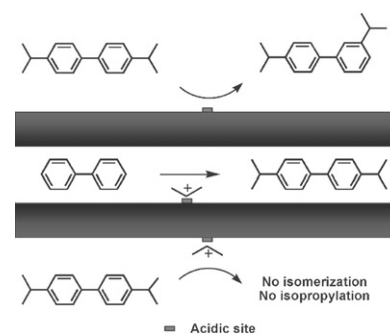


Yoshihiro Sugi, Ikuyo Toyama, Hiroshi Tamada, Shogo Tawada, Kenichi Komura, Yoshihiro Kubota

Journal of Molecular Catalysis A: Chemical 304 (2009) 22

The isomerization of 4,4'-diisopropylbiphenyl at external acid sites of H-mordenite during the isopropylation of biphenyl

The roles of external and internal acid sites of H-mordenite in the isopropylation of biphenyl (BP) on selectivities for 4,4'-diisopropylbiphenyl (4,4'-DIPB) was studied by changing catalyst amount and/or reaction temperature. Shape-selective catalysis occurs inside channels irrespective of reaction conditions. The decrease in selectivities for 4,4'-DIPB occurred by using large catalyst amounts and/or at higher temperatures is due to the isomerization of 4,4'-DIPB to 3,4'- and 3,3'-DIPB at external acid sites.

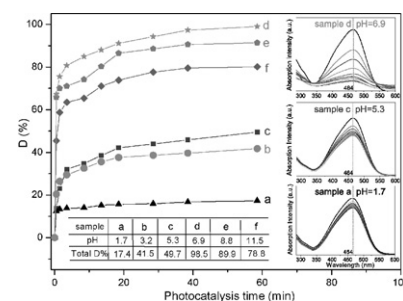


Aiping Zhang, Jinzhi Zhang, Naiyi Cui, Xiaoyun Tie, Yanwei An, Lingjie Li

Journal of Molecular Catalysis A: Chemical 304 (2009) 28

Effects of pH on hydrothermal synthesis and characterization of visible-light-driven BiVO_4 photocatalyst

Visible-light-driven BiVO_4 photocatalyst was hydrothermally synthesized at different pHs and exhibited changed morphologies, components and photocatalysis regularly. It reveals that monoclinic BiVO_4 shows better photocatalytic activities than tetragonal phase when evaluated by the decolorization of methyl orange in aqueous solution under visible light irradiation; and dispersive particles also represent higher activities than coagulate ones regarding of their photocatalysis.

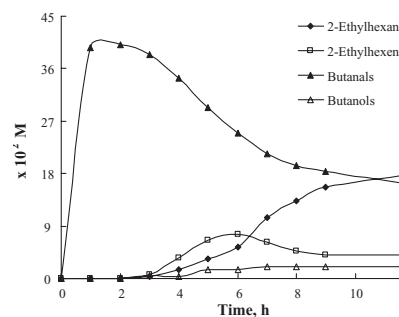


Sumeet K. Sharma, Ram S. Shukla, Parimal A. Parikh, Raksh V. Jasra

Journal of Molecular Catalysis A: Chemical 304 (2009) 33

The multi-step reactions for the synthesis of C_8 aldehydes and alcohol from propene in a single pot using an eco-friendly multi-functional catalyst system: Kinetic performance for parametric optimization

Kinetics of multi-step reactions including hydroformylation, aldol condensation and hydrogenation was studied for the synthesis of C_8 aldehydes and alcohol from propylene in a single pot using $[\text{HF}/\text{HT}]$ as a multi-functional heterogeneous catalyst. The rates of hydroformylation and aldol condensation with $[\text{HF}/\text{HT}(3.5)]$ were observed to be 2.5 and ~ 3 times respectively, higher than those associated with $[\text{HF}+\text{KOH}]$.

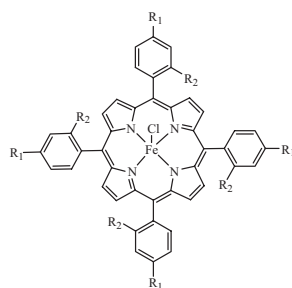


Nian Liu, Guo-Fang Jiang, Can-Cheng Guo, Ze Tan

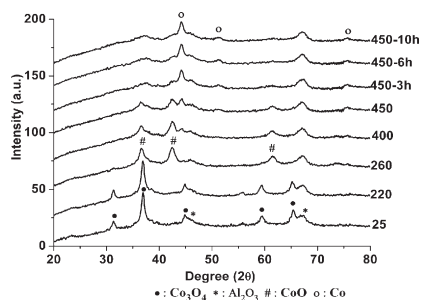
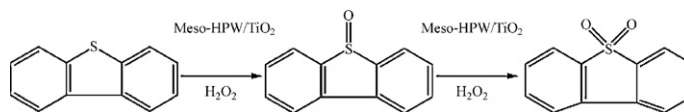
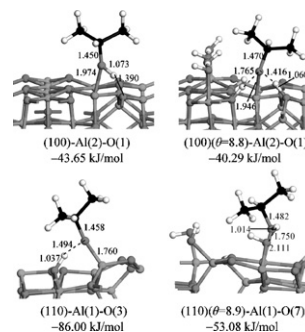
Journal of Molecular Catalysis A: Chemical 304 (2009) 40

Quantitative structure-activity relationship studies on ironporphyrin-catalyzed cyclohexane oxidation with PhIO

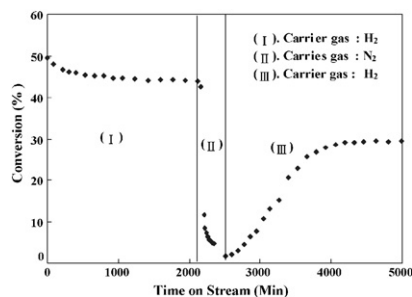
QSAR studies had been applied to investigate the cyclohexane hydroxylation reaction catalyzed by nine ironporphyrin derivatives. The ironporphyrin molecular structures' optimization and quantum chemical descriptors have been obtained based on quantum chemical calculations. Bi-parametric QSAR model equations for the rate constant $\lg k$ and cyclohexanol yield had been built separately by the MLR analysis.



- | | | |
|---|---------------------------|------------------------|
| 1 | $\text{R}_1=\text{H}$ | $\text{R}_2=\text{Cl}$ |
| 2 | $\text{R}_1=\text{F}$ | $\text{R}_2=\text{H}$ |
| 3 | $\text{R}_1=\text{Cl}$ | $\text{R}_2=\text{H}$ |
| 4 | $\text{R}_1=\text{Br}$ | $\text{R}_2=\text{H}$ |
| 5 | $\text{R}_1=\text{I}$ | $\text{R}_2=\text{H}$ |
| 6 | $\text{R}_1=\text{CH}_3$ | $\text{R}_2=\text{H}$ |
| 7 | $\text{R}_1=\text{OCH}_3$ | $\text{R}_2=\text{H}$ |
| 8 | $\text{R}_1=i\text{-Pr}$ | $\text{R}_2=\text{H}$ |
| 9 | $\text{R}_1=\text{NO}_2$ | $\text{R}_2=\text{H}$ |

Agudamu Bao, Kongyong Liew, Jinlin Li*Journal of Molecular Catalysis A: Chemical* 304 (2009) 47Fischer–Tropsch synthesis on CaO-promoted Co/Al₂O₃ catalystsAddition of small amount of calcium oxide promotes cobalt reducibility on alumina supported Fischer–Tropsch synthesis catalyst resulting in increased CO conversion and C₅⁺ selectivity while methane selectivity decreased slightly.**Xue-Min Yan, Ping Mei, Jiaheng Lei, Yuanzhu Mi, Lin Xiong, Liping Guo***Journal of Molecular Catalysis A: Chemical* 304 (2009) 52Synthesis and characterization of mesoporous phosphotungstic acid/TiO₂ nanocomposite as a novel oxidative desulfurization catalystMesoporous phosphotungstic acid/TiO₂ (HPW/TiO₂) nanocomposites, prepared by evaporation-induced self-assembly method, presents high catalytic active and selectivity in oxidative desulfurization of model fuel composed of dibenzothiophene (DBT) and hydrocarbon.**Gang Feng, Chun-Fang Huo, Chun-Mei Deng, Long Huang, Yong-Wang Li, Jianguo Wang, Haijun Jiao***Journal of Molecular Catalysis A: Chemical* 304 (2009) 58Isopropanol adsorption on γ -Al₂O₃ surfaces: A computational study**Ying-Chieh Yang, Hung-Shan Weng***Journal of Molecular Catalysis A: Chemical* 304 (2009) 65The role of H₂ in n-butane isomerization over Al-promoted sulfated zirconia catalyst

Findings show relatively stable catalytic activity of the Al/SZ catalyst at 250 °C when hydrogen is present because of hydrogen reaction with coke. In addition, the fouled catalyst regenerates by hydrogen provided the catalyst is not fully deactivated. Hydrogen adsorption reaction on Brønsted acid sites with deposited coke precedes regeneration.

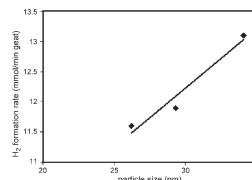


L. Li, Z.H. Zhu, S.B. Wang, X.D. Yao, Z.F. Yan

Journal of Molecular Catalysis A: Chemical 304 (2009) 71

Chromium oxide catalysts for CO_x-free hydrogen generation via catalytic ammonia decomposition

Mesoporous chromium oxide catalysts have been synthesized and evaluated for ammonia decomposition. The NH₃ decomposition on the Cr₂O₃ catalysts is structure-sensitive and the most active catalyst has a large particle size. Moreover, interstitial CrN_xO_y compounds have been found to act as the active sites for the NH₃ decomposition.

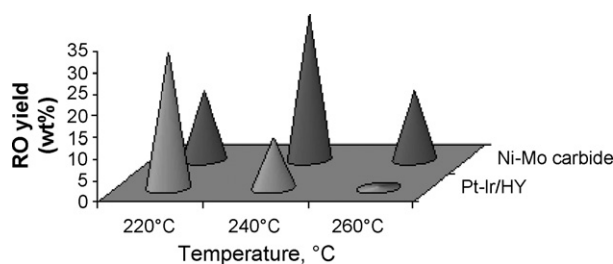


K. Chandra Mouli, V. Sundaramurthy, A.K. Dalai

Journal of Molecular Catalysis A: Chemical 304 (2009) 77

A comparison between ring-opening of decalin on Ir-Pt and Ni-Mo carbide catalysts supported on zeolites

Ring-opening of decalin was studied on Pt-Ir and Ni-Mo carbide catalysts supported on HY and Hbeta. 33.7 wt.% and 40 wt.% of ring-opening yield and selectivity were observed on Ni-Mo carbide/HY catalyst at 240 °C, whereas 31.7 wt.% and 65 wt.% of ring-opening yield and selectivity were observed on Pt-Ir/HY catalyst at 220 °C. Therefore, the Ni-Mo carbide catalysts can be successfully used to obtain the same level of the ring-opening yields that can be achievable by using noble metal catalysts.

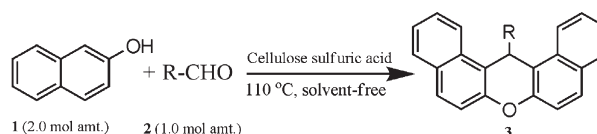


J. Venu Madhav, Y. Thirupathi Reddy, P. Narsimha Reddy, M. Nikhil Reddy, Suresh Kuarm, Peter. A. Crooks, B. Rajitha

Journal of Molecular Catalysis A: Chemical 304 (2009) 85

Cellulose sulfuric acid: An efficient biodegradable and recyclable solid acid catalyst for the one-pot synthesis of aryl-14H-dibenzo[*a,j*]xanthenes under solvent-free conditions

Aryl-14H-dibenzo[*a,j*]xanthenes are synthesized via the condensation of β-naphthol with different aromatic aldehydes using an efficient, biodegradable, eco-friendly, reusable solid support acid catalyst cellulose sulfuric acid as a catalyst under solvent-free conditions.

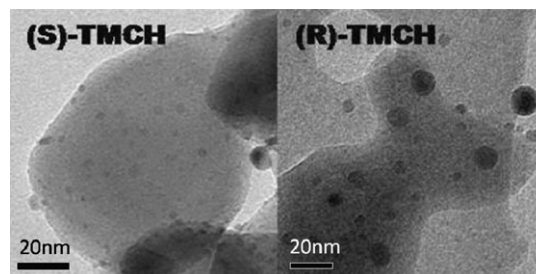


Shuang Li, Chunhui Chen, Ensheng Zhan, Shang-Bin Liu, Wenjie Shen

Journal of Molecular Catalysis A: Chemical 304 (2009) 88

Chirality inversion in enantioselective hydrogenation of isophorone over Pd/MgO catalysts in the presence of (*S*)-proline: Effect of Pd particle size

The configuration of the chiral product in enantioselective hydrogenation of isophorone is strongly dependent on the size of Pd particle. Pd particles smaller than 4 nm favor a primary hydrogenation of isophorone to TMCH, followed by a kinetic resolution giving (*S*)-TMCH. Pd particles larger than 10 nm produce (*R*)-TMCH through the hydrogenation of isophorone–proline adduct.

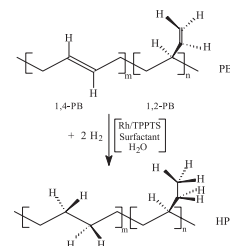


Vasilis Kotzabasakis, Nikos Hadjichristidis, Georgios Papadogianakis

Journal of Molecular Catalysis A: Chemical 304 (2009) 95

Catalytic conversions in aqueous media: Part 3. Biphasic hydrogenation of polybutadiene catalyzed by Rh/TPPTS complexes in micellar systems

Water-soluble Rh/TPPTS complexes [TPPTS = P(C₆H₄-*m*-SO₃Na)₃] are active catalysts (TOF > 1200 h⁻¹) for the biphasic hydrogenation of the completely water-insoluble heavy polybutadiene (PB) in single micelles formed by the cationic surfactant dodecyltrimethylammonium chloride (DTAC), or mixed micelles created by DTAC with either non-ionic or anionic surfactants. The hydrogenation rate depends critically on the microstructure of PB and the nature of micellar catalysis. The 1,4-units content of PB plays a major role for performing the catalytic hydrogenation reaction in single or mixed micellar systems for obtaining maximum reactivity.



Praveen K. Tandon, Manish Srivastava, Santosh Kumar, Satpal Singh

Journal of Molecular Catalysis A: Chemical 304 (2009) 101

Iridium(III) catalyzed oxidation of toluene and ethyl benzene by cerium(IV) in aqueous acidic medium

Rate of the reaction in oxidant is first order in the beginning, reaches to a maximum and then starts decreasing. Oxidation is selective to benzaldehyde in toluene and to acetophenone in ethyl benzene.

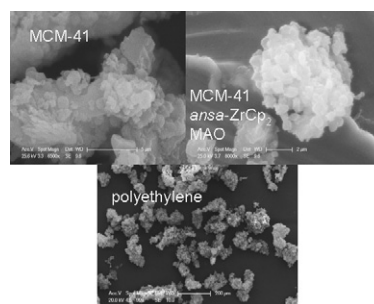
$$\text{Rate} = \frac{k K_1 K_2 [\text{Ce}^{\text{IV}}][\text{S}][\text{Ir}^{\text{III}}]_{\text{T}}}{[\text{Ce}^{\text{III}}][\text{H}^+] + K_1 K_2 [\text{Ce}^{\text{IV}}][\text{S}]}$$

Carlos Alonso-Moreno, Damián Pérez-Quintanilla, Dorian Polo-Cerón, Sanjiv Prashar, Isabel Sierra, Isabel del Hierro, Mariano Fajardo

Journal of Molecular Catalysis A: Chemical 304 (2009) 107

MCM-41/*ansa*-zirconocene supported catalysts: Preparation, characterization and catalytic behaviour in ethylene polymerization

The preparation and structural characterization of *ansa*-zirconocene complexes supported on MCM-41 is described. The behaviour of these supported catalysts in the polymerization of ethylene has been studied and compared with their silica gel analogues.

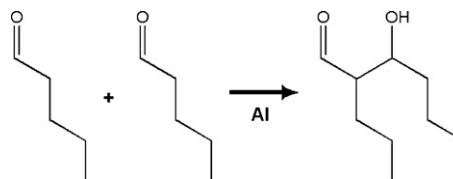


Andrew S. Heintz, Javier E. Gonzales, Mark J. Fink, Brian S. Mitchell

Journal of Molecular Catalysis A: Chemical 304 (2009) 117

Catalyzed self-aldol reaction of valeraldehyde via a mechanochemical method

The self-aldol reaction of valeraldehyde to 2-propyl-3-hydroxyl-heptanal is catalyzed by fresh aluminum surface created during high-energy ball milling.

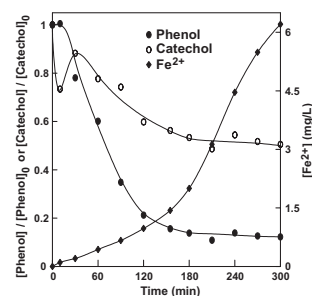


**Chun-Ping Huang, Chang-Ren Chen,
Yi-Fong Huang, Yu-Wen Lu, Yao-Hui Huang**

Journal of Molecular Catalysis A: Chemical 304 (2009) 121

Reductive dissolution and oxidative catalysis of an immobilized iron oxide in the presence of catechol and phenol

An original study of an immobilized iron oxide catalyst (SiG1) with one hydroxylation intermediate of aromatic compounds (catechol) in the reductive dissolution process was performed. Also, SiG1 was applied as the catalyst for the oxidation of phenol and catechol in the presence of hydrogen peroxide. Catechol induced the reductive dissolution of SiG1 and then promoted its own oxidation along with that of phenol in the presence of H_2O_2 .

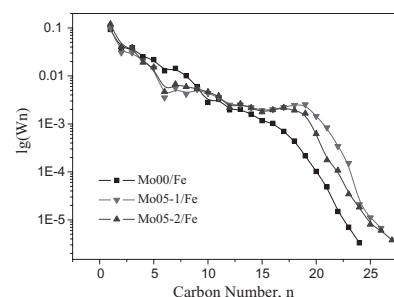


**Shaodong Qin, Chenghua Zhang, Jian Xu,
Baoshao Wu, Hongwei Xiang, Yongwang Li**

Journal of Molecular Catalysis A: Chemical 304 (2009) 128

Effect of Mo addition on precipitated Fe catalysts for Fischer–Tropsch synthesis

Molybdenum modified participated Fe catalysts were prepared by two different ways. Mo addition markedly enhanced C_{12}^+ hydrocarbon selectivity, while suppressed C_2 – C_8 hydrocarbon selectivity. The overall hydrocarbon product distribution apparently deviates from the Anderson–Schulz–Flory (ASF) kinetics, which is probably due to the acidic sites of Mo oxides promoting the olefin readsorption and secondary reaction.

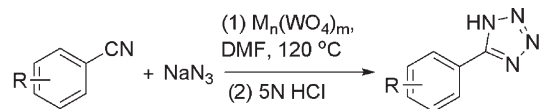


**Jinghui He, Baojun Li, Fasheng Chen, Zheng Xu,
Gui Yin**

Journal of Molecular Catalysis A: Chemical 304 (2009) 135

Tungstates: Novel heterogeneous catalysts for the synthesis of 5-substituted 1H-tetrazoles

We report that tungstate MWO_4 ($M = Ba, Ca, Zn, Cd, Cu, Na, H$) can catalyze the [2+3] cycloaddition reaction of nitriles with sodium azide to produce 5-substituted 1H-tetrazoles in DMF solution. The catalyst is very efficient with good yield for aromatic nitriles. The mono- and di-addition products from dicynaobenzene can be selectively synthesized.



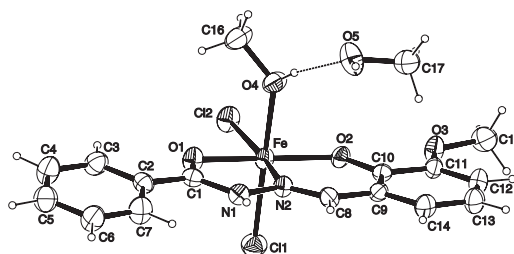
$R = H, Cl, NO_2, CN.$ $M = Ba, Cu, Zn, Cd,$ Yields: moderate
 $Ca, Na, H.$ to good.

**Hassan Hosseini Monfared, Somayeh Sadighian,
Mohammad-Ali Kamyabi, Peter Mayer**

Journal of Molecular Catalysis A: Chemical 304 (2009) 139

Iron(III) aroylhydrazone complexes: Structure, electrochemical studies and catalytic activity in oxidation of olefins

Tridentate Schiff base ligands derived from aromatic aldehydes and benzhydrazide, and their iron complexes $[\text{Fe}(\text{L}^1)(\text{HL}^1)]$ **1**, $[\text{Fe}(\text{HL}^1)\text{Cl}_2(\text{CH}_3\text{OH})] \cdot (\text{CH}_3\text{OH})$ **2** and $[\text{Fe}(\text{HL}^2)\text{Cl}_2(\text{H}_2\text{O})]$ **3** have been prepared and characterized. The crystal structure of **2** has been determined. Electrochemical studies have revealed quasi-reversibility for these compounds. The catalytic potential of these complexes has been tested for the oxidation of olefins using *tert*-butylhydroperoxide (TBHP) as oxidant.

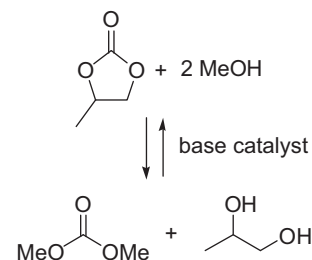


**D. Bradley G. Williams, Mike S. Sibiya,
Pieter S. van Heerden, Megan Kirk,
Roger Harris**

Journal of Molecular Catalysis A: Chemical 304 (2009) 147

Verkade super base-catalysed transesterification of propylene carbonate with methanol to co-produce dimethyl carbonate and propylene glycol

Verkade super bases are excellent transesterification catalysts for the conversion of propylene carbonate into dimethyl carbonate and propylene glycol at low catalyst loadings. Batch data and *in situ* generated NMR data correlate well and the kinetics of the reaction are studied.

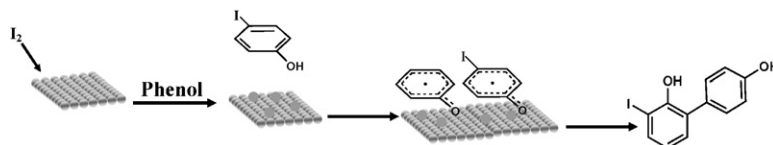


**A. Murugadoss, Papori Goswami, Anumita Paul,
Arun Chattopadhyay**

Journal of Molecular Catalysis A: Chemical 304 (2009) 153

'Green' chitosan bound silver nanoparticles for selective C-C bond formation via *in situ* iodination of phenols

Ag nanoparticles (NPs) embedded in a composite with 'green' chitosan could catalyze C-C coupling reaction of phenols (*ortho-para*) in the presence of iodine, in a short time and at room temperature, with high selectivity and yield.

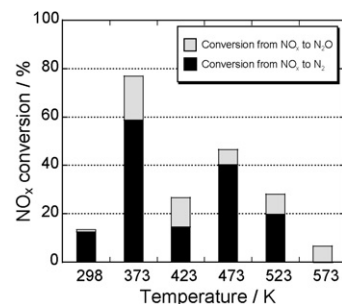
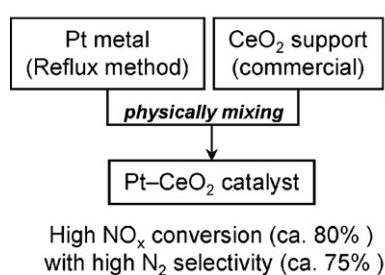


**Masahiro Itoh, Makoto Saito, Masahiko Takehara,
Koji Motoki, Jun Iwamoto, Ken-ichi Machida**

Journal of Molecular Catalysis A: Chemical 304 (2009) 159

Influence of supported-metal characteristics on deNO_x catalytic activity over Pt/CeO₂

Good deNO_x activity was observed on the catalyst prepared by physically mixing the fine Pt metal particles with the CeO₂ support due to the suitable metal-support interaction and specific catalytic activity of Pt metal particles.

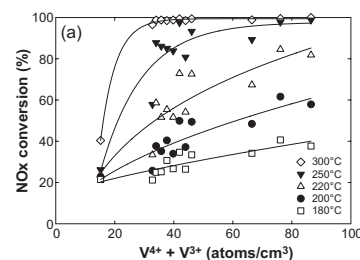


**Sang Hyun Choi, Sung Pill Cho, Jun Yub Lee,
Sung Ho Hong, Sung Chang Hong,
Suk-In Hong**

Journal of Molecular Catalysis A: Chemical 304 (2009) 166

The influence of non-stoichiometric species of V/TiO₂ catalysts on selective catalytic reduction at low temperature

Vanadium-supported titania catalysts are comprised of not only Ti⁴⁺ but also Ti³⁺ and Ti²⁺ called non-stoichiometric Ti^{y+} ($y \leq 3$), while the vanadium-free titania support consists of only Ti⁴⁺. Moreover V has various valence states such as V⁵⁺ and V^{x+} ($x \leq 4$), which contains V⁴⁺, V³⁺, etc. The SCR catalytic activity increases with increasing the amount of non-stoichiometric species per unit volume.

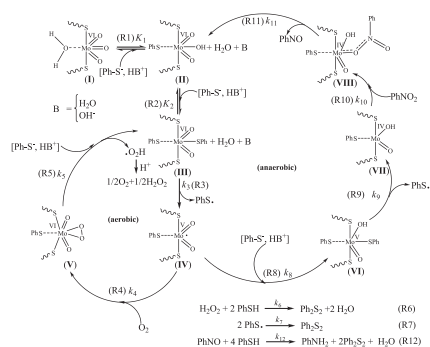


Antonio Ribera, Francisco Pérez-Pla, Elisa Llopis, Antonio Cervilla, Antonio Domenech

Journal of Molecular Catalysis A: Chemical 304 (2009) 174

A kinetic model for the oxidation of benzenethiol catalyzed by the $[\text{Mo}^{\text{VI}}\text{O}_2(\text{O}_2\text{CC}(\text{S})(\text{C}_6\text{H}_5)_2)_2]^{2-}$ complex intercalated in a Zn(II)–Al(III) layered double hydroxide host

A kinetic model for the oxidation of benzenethiol catalyzed by the $[\text{Mo}^{\text{VI}}\text{O}_2(\text{O}_2\text{CC}(\text{S})(\text{C}_6\text{H}_5)_2)_2]^{2-}$ complex intercalated in a Zn(II)–Al(III) layered double hydroxide host have been investigated under aerobic conditions.

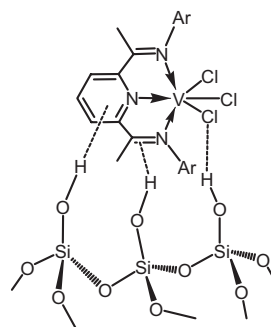


Javier Romero, Fernando Carrillo-Hermosilla, Antonio Antiñolo, Antonio Otero

Journal of Molecular Catalysis A: Chemical 304 (2009) 180

Homogeneous and supported bis(imino)pyridyl vanadium(III) catalysts

Bis(imino)pyridyl vanadium (III) complexes have been synthesized and characterized. The reactivity of these complexes as precursors of homogeneous and supported ethylene polymerization catalysts was evaluated.

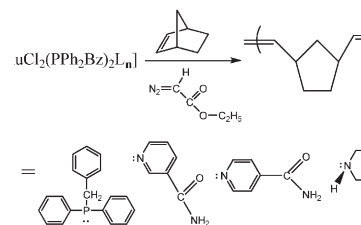


José L. Silva Sá, Benedito S. Lima-Neto

Journal of Molecular Catalysis A: Chemical 304 (2009) 187

Ability of Ru complexes for ROMP tuned through a combination of phosphines and amines

Different Ru(II) complexes show distinct reactivities for ROMP of norbornene on account of a combination of synergistic effects of the ancillary ligands. The propagating species are hybrid amine–phosphine complexes. For example, $[\text{RuCl}_2(\text{PPh}_2\text{Bz})_3]$ was not active at room temperature, whereas $[\text{RuCl}_2(\text{PPh}_2\text{Bz})_2(\text{piperidine})]$ showed 92% yield for 30 min at 25 °C with $[\text{NBE}]/[\text{Ru}] = 5000$.



V. Arun, N. Sridevi, P.P. Robinson, S. Manju, K.K.M. Yusuff

Journal of Molecular Catalysis A: Chemical 304 (2009) 191

Ni(II) and Ru(II) Schiff base complexes as catalysts for the reduction of benzene

Two new complexes $[\text{M}^{\text{II}}(\text{L})(\text{Cl})(\text{H}_2\text{O})_2] \cdot \text{H}_2\text{O}$ (where M = Ni or Ru and L = heterocyclic Schiff base, 3-hydroxyquinoxaline-2-carboxalidene-4-aminoantipyrine) have been synthesized and characterized. These complexes were shown to be efficient catalysts for the reduction of benzene. The nickel complex shows more selectivity for the formation of cyclohexene while the ruthenium complex is more selective for the formation of cyclohexane.

